Numerical Simulation of solitary waves propagating on stepped slopes beaches

FAYÇAL CHERGUI[1] , MOHAMED BOUZIT[2]
[1]Marine Engineering Department ; [2]Mecanical Engineering Department
University of Science and Technology of Oran Mohamed Boudiaf
El Mnaouar, BP 1505, Oran, Bir El Djir
ALGERIA

Abstract: - The objective of the current paper is to study the propagating and breaking of solitary waves on stepped slopes beaches, to simulate the shoaling and breaking, specifically the location of breaking point *Xb*, and solitary wave height at breaking *Hb* of solitary waves on the different stepped slopes. Ansys Fluent is used to implement the simulation, a two-dimensional volume of fluid (VOF) which is based on the Reynolds-Averaged Navier–Stokes (RANS) equations and the k–ε turbulence closure solver. The obtained results were firstly validated with existing empirical formulas for solitary wave run-up on the slope without stepped structure and are compared with the experimental and numerical results. The numerical computation has been carried out for several, configurations of beach slopes with tan β*= 1:15, 1:20, 1:25*, wave height H_0*= 0.04, 0.06, 0.08m*, water depth h_0*= 0.15, 0.2, 0.25m*, and step height S_h*= 0.025, 0.05, 0.075m*. A set of numerical simulations were implemented to analyze shoaling and breaking of solitary waves, wave reflection, wave transmission, and wave run-up with various parameters wave heights, water depth, beach slopes, and S_h step height.

Key-Words: Solitary waves - Breaking point - Wave run-up - Stepped slope - Navier−Stokes equations

Received: May 25, 2021. Revised: April 13, 2022. Accepted: May 11, 2022. Published: June 28, 2022.

1 Introduction

Long waves such as tsunamis and waves resulting from large displacements of water caused by phenomena such as landslides and earthquakes sometimes behave approximately like solitary waves. The run-up, overturn, and breaking of solitary waves are the most direct ways to damage the constructions near the offshore, the most famous are tsunamis. Indeed, since the giant tsunami that occurred in the Indian Ocean on 26 December 2004 caused memorable losses [1], this phenomenon has aroused particular interest, and it's necessary to understand their dynamics more clearly to predict them more efficiently. The first to start theoretical studies of solitary waves [2,3,4,5] , more recent analyses of solitary waves have been performed [6,7,8].

At present, numerical models for tsunami wave simulations were mainly carried out. In most cases, solitary waves were used to represent a tsunami wave, in general, solitary waves were used to represent a tsunami wave [9,10,11,12,13]. The breaking factor plays an important role in the calculation of wave heights, some researchers have attempted to define breaking factors for the run-up of a solitary wave on plane slopes.

In the literature, the two-dimensional simulation of wave induced free surface flows can carried out by numerical models that integrate the two-dimensional Navier- Stokes equations [14] , Ji et al.[15] and Hieu et al.[16] Presented a numerical two-phase flow model coupling with the VOF method, including the processes of wave shoaling, wave breaking, wave reflection,

and air movement, compared the simulation of wave breaking on a sloping bottom with the conditions of the experiment by Ting et al.[17]. Dentale et al.[18] Evaluated the filtration of the fluid within the interstices of a concrete blocks breakwater by integrating the Reynolds Averaged Navier-Stokes equations (RANS) inside the voids. Khaware et al.[19] Investigates the sensitivity of 5th order solitary wave models are applied to shallow wave scenarios with high relative heights, modeling from both an analytical and a numerical perspective, using a (VOF) method, coupled with the Open Channel Flow module in ANSYS Fluent, it has been shown that the Stokes wave theory can be applied in the shallow regime and concluded that the Explicit formulation is very sensitive near breaking conditions requirement of very small time step size. The turbulence model most commonly used is the standard k–ε model, Hsiao et al.[9] studied experimentally and numerically of wave tsunami-like solitary waves impinging and overtopping an impermeable trapezoidal seawall on a *1:20* sloping beach, Reynolds-Averaged Navier–Stokes (RANS) equations are used to describe mean flow fields, and the modified *k-ε* closure model is employed to examine turbulence behaviors. Wu et al.[20] compared the tsunami force on structure using different *k-ε* turbulence models and pointed out that the *k-ε* RNG model has higher calculation accuracy.

The research on the propagation, shoaling and breaking of solitary waves were mainly carried out. [21] has computed shoaling and breaking of solitary waves on slopes, discussed the characteristics of various breaking types and made a clear classification of wave breaking, they proposed a set of empirical formulae for breaking criterion, as shown in Eq. (11), who S is the breaking coefficient of the solitary wave, which can be used to determine the wave breaking type. According on Eq. (11), the value of the breaking coefficient S for the cases in this study can be calculated the results show $0.1 < S < 0.26$, that indicates that the wave breaking type of all the cases in this study is plunging breaking (PL). Hsiao et al.[22] simulated the shoaling and breaking of solitary waves on a beach , and re-examined some of a set of empirical formulae of Grilli et al. [21] the experimental results agree well. Akbari et al.[23] Improved (SPH) method to study solitary wave overtopping for different coastal structures, and model are verified by simulating solitary wave breaking over a sloping bed, based on laboratory data presented by Grilli et al. [21]. Gallerano et al.[24] propose a modified turbulence model to represent the energy dissipation due to the wave breaking.

Numerous studies are focusing on the run-up of solitary waves, Wu et al.[25], Chou et al.[26] and Lin et al.[27] indicated that the run-up height increases with beach slope for breaking solitary waves. Kuai et al.[28] Realized experimental measurements demonstrate the effect of the impact of the jet from a plunging breaking solitary wave and the post breaking bore formed on the resultant run-up showing spatial snapshots in detail on *1:15* slope for incident wave height $H/h_o = 0.40$. [29] Presented numerical investigations of the run-up and hydrodynamic characteristics of solitary waves influenced by beach slope, concludes the run-up heights of breaking solitary waves increase with beach slope. Yao et al.[29] Investigated numerically the reduction of tsunami-like solitary wave run-up by the pile breakwater on a different sloping beach, the adopted model was validated with existing empirical formulas Synolakis et al. [30] and Hsiao et al. [22] for solitary wave run-up on the slope without the pile structure.

Other protection systems have been studied, such as stepped form, which combines needs in current coastal protection by increasing the surface roughness of the coastal protection structure to reduce wave run-up and wave overtopping. A comprehensive literature review by Kerpen et al.[31] detailed discusses previous studies on stepped revetments as a coastal protection measure. Experimental studies are carried out by Kerpen et al.[32] for the empirical derivation of a roughness reduction coefficient for wave overtopping on stepped revetments in relation to a smooth slope, mentioned the importance of the dimensionless

step height on the energy dissipation in the wave run-up and, as a consequence, the reduction of the mean overtopping discharge. Shih et al.[33] investigated the energy dissipation characteristics of stepped obstacles in a physical wave flume, varying the angle of the stepped surface with the slope of the embankment surface, with various interaction angles between the incident waves and the rough stepped surfaces.

In the present study, the propagating solitary waves on stepped slope beach was numerically studied for the different wave height, beach slopes, water depth, and step height. The unsteady Reynolds averaged Navier-Stokes (RANS) equations coupled with a k-ε turbulence model are applied to simulate the free surface elevation. The main purpose of this study is to numerically simulate the shoaling and breaking, specifically the location of breaking point *Xb*, and solitary wave height at breaking *Hb* of solitary waves on the different stepped slope and investigate the run-up, the wave reflection, and the wave transmission of solitary waves influenced by the incident wave height, beach slope, water depth, and step height Sh.

2 Numerical model

2.1 Governing equations

Two dimensional Reynolds Averaged Navier Stokes (RANS) are numerically solved in the CFD solver FLUENT [34,35], to simulate the unsteady and incompressible viscous fluids, in which the continuity equation and the momentum equation are, respectively:

$$\frac{\partial u_i}{\partial x_i} \quad (1)$$

$$\frac{\partial(\rho u_i)}{\partial t} + \frac{\partial(\rho u_i u_j)}{\partial x_j} = -\frac{\partial P}{\partial x} + \frac{\partial}{\partial x_j}\left(\mu \frac{\partial u_i}{\partial x_j} - \overline{\rho u_i' u_j'}\right) \quad (2)$$

Where *i* and *j* are the cyclic coordinates in an orthogonal coordinate system whose values are 1 and 2, while u_i are the time-averaged velocity components; ρ is the density of the fluid; p is the pressure.

In this study, the *k-ε* turbulence model proposed by (Launder and Spalding., 1972) are selected [20,34,36] , which are as following:

$$\frac{\partial}{\partial t}(\rho k) + \frac{\partial}{\partial x_i}(\rho k u_i) = \frac{\partial}{\partial x_j}\left[\left(\mu + \frac{\mu_t}{\sigma_k}\right)\frac{\partial k}{\partial x_j}\right] + G_k - \rho\varepsilon \quad (3)$$

$$\frac{\partial}{\partial t}(\rho \varepsilon) + \frac{\partial}{\partial x_i}(\rho \varepsilon u_i) = \frac{\partial}{\partial x_j}\left[\left(\mu + \frac{\mu_t}{\sigma_\varepsilon}\right)\frac{\partial \varepsilon}{\partial x_j}\right] + C_{1\varepsilon}\frac{\varepsilon}{k}G_k - \rho C_{2\varepsilon}\frac{\varepsilon^2}{k} \quad (4)$$

To identified interfaces between non-penetrating fluids a Volume of Fluid Method (VOF) is used by Khaware et al.[19] and Zhan et al.[36]. The volume fraction of a specific fluid (α) is defined as the ratio of the volume of that fluid to total volume. Interfaces between different fluids are identified by volume fraction falling between 0 and 1.

Summation of volume fraction for all the fluids should be equal to one

$$\sum_a \alpha = 1 \quad (5)$$

Volume fraction equation is given as,

$$\frac{\partial \alpha}{\partial t} + \nabla.(\bar{u}\alpha) = 0 \quad (6)$$

Total continuity equation for incompressible fluid is given as,

$$\nabla.\bar{u} = 0 \quad (7)$$

To solve this model, the PISO scheme is used for pressure velocity coupling [19], second-order upwind and compressive schemes are used for momentum and volume fraction respectively. First-order transient methods are used allowed with Explicit formulation. Finally, first-order upwind scheme was selected for the discretization of the equations of turbulent energy and dissipation.

2.2 Wave generation and solitary wave theory

Fluent formulates the Solitary wave theories that are expressed using Jacobian and elliptic functions based on the work by D. John Fenton et al., 1998 [37]. These wave theories are valid for high steepness finite amplitudes waves operating in intermediate to deep liquid depth range.
The generalized expression for wave profile for 5th order Stokes theory is given as.

$$\varsigma(X,t) = \frac{1}{k}\sum_{i=1}^{5}\sum_{j=1}^{i} b_{ij}\xi^{i}cos\big(jk(x-ct)\big) \tag{8}$$

$$\xi = \frac{kH}{2} = \frac{\pi H}{L} \;\; and \; k = \frac{2\pi}{L}$$

$$c = \sqrt{\frac{g}{k}\tanh(kh)}\left(\sum_{i=1}^{5} c_i\xi^{i}\right) \tag{9}$$

Where c is wave celerity and k is wave number, b_{ij} c_i , are complex expressions of kH.

Solitary wave theories are more widely used for shallow depth regimes, are derived by assuming that the waves have infinite wave length. 5th order solitary wave expressions are complex functions of relative height (H/h).

Wave profile for a shallow wave is defined as

$$\varsigma(X,t) = H\, sech^2\left[\frac{k}{h}(x - x_0 - ct)\right] \tag{10}$$

where wave celerity and wave numbers are given as

$$c = \sqrt{gh}\left(1 + \frac{H}{2h}\right) \;\; and \;\; k = \frac{1}{h}\sqrt{\frac{3H}{4h}}$$

and x_0 is the initial position of wave

3 Numerical setup

3.1 Numerical domain

The computational domain for the propagation of solitary waves is shown in Fig. 1(a) two-dimensional numerical wave flume is built, the flume is with the total length of 15.5 m, height of 0.4 m, the numerical waves were set to be generated at 7 m seaside of the slope toe.

The free surface elevation along the flume was measured by nine numerical wave gauges Fig. 1(a) with x=0 denotes the slope toe, which (ng01) was placed -3m upstream of the slope, (ng02) at the slope toe, (ng03) at 0.75m, (ng04) at the middle of the stepped structure 1.5m (stepped width), and (ng05) at end of the stepped structure 3m, for the others are placed downstream the stepped structure spaced 0.5m until (ng09) where is placed at 4.5m downstream the toe of the slope. H_0 is the incident wave height; h_0 is the still water depth at the plane bed, β is the angle of beach slope.

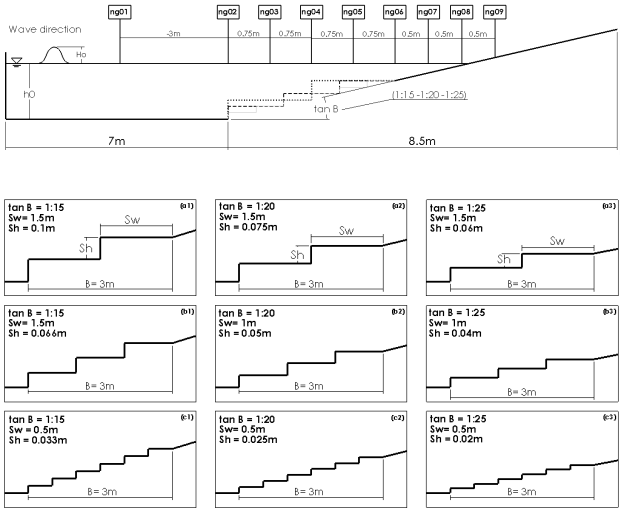

Fig. 1 (a) Schematic view of the numerical wave flume, with x=0 denotes the slope toe;
(b) Schematic view of the stepped structure on slope.

The stepped structure are installed along of slope just 3m in front of the toe Fig. 1(b), three cases of stepped structure are studied *Sw=0.5m, 1m*, *1.5m* (*Sw* is step width, *Sh* is step height and B is stepped width fixed 3m) for three different slopes (*tan β = 0.15, 0.20, 0.25)* , then we have a total of nine cases of stepped structure.

3.2 Boundary Conditions and mesh description

The wave propagates from the left where solitary waves are generated in the inlet boundary to the right where no-slip wall boundary condition is applied. The bottom and stepped structure are considered a no-slip wall and the top is considered a pressure outlet.

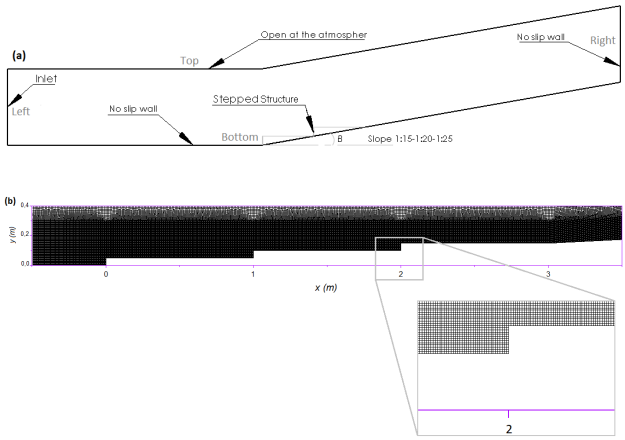

Fig. 2 (a) Layout of the numerical setup; (b) Numerical grids of the computational domain.

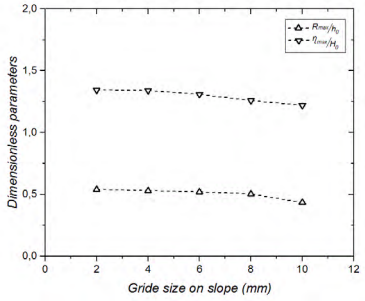

Fig. 3 Variations of the normalized η_{max}/H_0 maximum free surface elevation of breaking point and R_{max}/h_0 maximum wave run-up on the slope with different grid sizes.

To validate the model, the structured mesh is applied Fig. 2(a). ANSYS ICEM is employed to build a geometric model and generate grids, a numerical convergence test was performed by varying the grid size on slope using the typical wave condition of $h_0 = 0.2\ m$ and $H_0 = 0.06\ m$. We also tested another four sizes (2, 6, 8 and 10 mm) Fig. (3) showing the results for the normalized maximum free surface elevation η_{max}/H_0 of breaking point and the normalized maximum runup R_{max}/h_0 on the slope. The differences in the simulations were generally 6.5% when the grid size is 10 mm, 4% grid size 8mm and 2.5% when the grid size declined from 4 mm to 2 mm.

In vertical direction, the grid size start from 4mm it was kept a constant all the way at 0.3m and 4mm to 8mm to the domain top. In the stream-wise direction, from the inlet of domain to the slope toe, the grid size reduced gradually from 8mm to 4mm, and were kept constant 4mm from the slope toe at a location 1m downstream of stepped structure, to capture the shoaling and breaking of solitary waves, and the grid size increased gradually from 4 mm to 8 mm at the end of domain. After conducting several simulations with various time step sizes, a time step size of $t= 0:001s$ was chosen to ensure the solution's accuracy and convergence, all the simulations have been carried out on a Core i7-3770, 3.40 GHz, and RAM 16.0 GB computer, the simulation was run for 12 s to guarantee the completion of wave run-up and rundown processes on the slope.

4 Results and Discussions

4.1 Model validation

Firstly, a numerical test was conducted without stepped structure to verify the solitary waves generated by the model at numerical wave gauge (ng01), we compared the experimental work and the numerical generated solitary wave profile with the theoretic profile calculated by the equation of Yao et al.[29] Fig. 4(a). Numerical results are in good agreement with theoretical solutions up to a relative height of $H_0= 0.06m$, except at the tail of solitary wave deviates compared to the experimental result.

We then compared the run-up of the four offshore solitary wave heights with a fixed offshore water depth of $h_0= 0.2m$. tested wave

conditions (H_0=*0.02, 0.04, 0.06, 0.08m*) with the laboratory experiments and the numerical simulations Fig. 4(b). It's observed that the formula's Hsiao et al. [22] predicted slightly less wave run-up than those predicted by Synolakis et al. [30] for the current laboratory slope of 1:20. The present result shows a slight increase that those shown by Yao et al.[29]. When the wave height increases, the slightly becomes more important. The maximum error of run-up value compared to laboratory experiments is approximately 2% for H_0= *0.02m*, 3%, for H_0=*0.04m*, 6% for H_0= *0.06m* and 10% for H_0=*0.08m*.

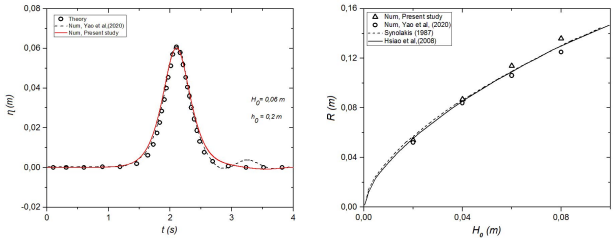

Fig. 4 (a) Comparison of the solitary wave profile of the numerical present results with numerical and the theory result; (b) Comparison of the maximum wave run-up R on the slope between the simulations and the predictions from the empirical formulas.

Similar experiments were also conducted by Hsiao et al. [9], except that a trapezoidal seawall was placed in the slope 1:20. A solitary wave with a wave height of H_0= *0.07m* in the water depth of h_0= *0.2m* was generated. Where a reference wave gauge (wg01) was fixed at 1.1 m in front of the beach slope, another wave gauge downstream of the slope, (wg03) placed 1.7m and (wg10) placed at 3.744m behind the slope toe. The simulation results are also compared, the comparison between the solitary wave profile obtained by the experimental and numerical simulation of (Hsiao et al., 2010), shows that the present computed results are a little different from the results Fig. 5**.**

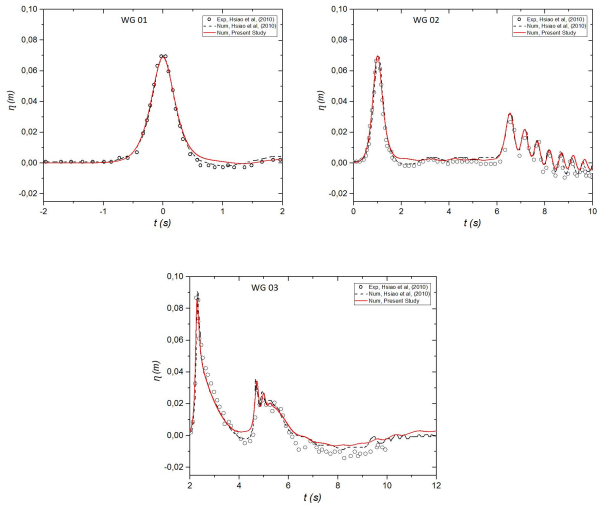

Fig. 5 Comparison of the solitary wave profile of the numerical present results with the experimental and numerical.

A breaking wave is a wave whose amplitude (H_b) reaches a maximum level (Breaking point BP) at which process can start to occur, the solitary breaking wave type can be categorized by using a slope parameter, So, suggested by Grilli et al. [21], as shown in Eq. (11).

$$S_0 = 1.521 \frac{\tan\beta}{\sqrt{\varepsilon}} \qquad (11)$$

In which tan β is the angle of beach slope, $\varepsilon = H_0/h_0$ is the wave steepness, H_0 is the wave height, h_0 is the water depth measured from the flat flume bottom and H_b is solitary wave height at breaking.

$$\frac{h_b}{h_0} = \frac{0.149}{(S_0/\varepsilon)^{0.523}} \quad with\ S_0 < 0.3 \qquad (12)$$

$$\frac{H_b}{h_0} = 0.841 \exp(6.421)\, S_0 \qquad (13)$$

The ranges of different breakers are $0.3<S_0<0.37$ for surging type (SU), $0.025<S_0<0.30$ for plunging type (PL) and $S_0<0.025$ for spilling type (SP) [21], the water depth (h_b) at breaking point can be estimated by Eq.(12).

From the equation (12) we can extract the theoretical values location of solitary wave breaking point X_b, and compared with the numerical value, as shown in Fig. 6, using the

typical wave condition of $h_0 = 0.2\ m$ and $H_0 = 0.02, 0.04, 0.06$ and $0.08\ m$ on 1:20 slope. it can be observed that the difference between the numerical and theoretical solution changes according to the wave height, the maximum difference is 0.2m.

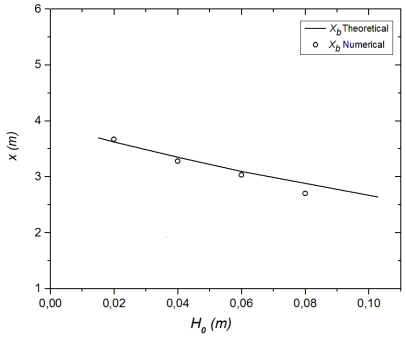

Fig. 6 The location of breaking point between present numerical solution and theoretical solution by Grilli et al. [21]

It can be seen that the numerical results agree well with the compared results, which demonstrates that the present model is capable of accurately simulating the propagation, the shoaling and breaking of solitary waves on slopes considerably well.

4.2 Wave surface elevations and breaking wave

The wave surface elevation time histories at the different gauges are presented Fig. 7, a numerical reference gauge (ng01) is placed at x=-3 m from the toe of the slope. It can be noted that the wave height of the solitary wave almost remains unchanged along the flat flume bottom (ng01) for all cases study, indicating that the numerical flume can simulate solitary wave propagation considerably well, and a slight increase observed (ng02).

It also can be shown for $Sh=0$ and $Sh= 0.025m$ that the wave height of the solitary wave becomes large gradually (ng06), but this is not the case for $Sh=0.05m$ and $Sh=0.075m$ the wave height decreases abruptly because the breaking point is closer behind the numerical wave gauge, as the figure Fig. 7 shows very well the breaking point phase of the wave, this means that as the step height Sh rises, so does the breaking point is further backward. The solitary wave steepens because of shoaling effect; and then the wave height decreases, indicating the solitary wave breaks (ng08).

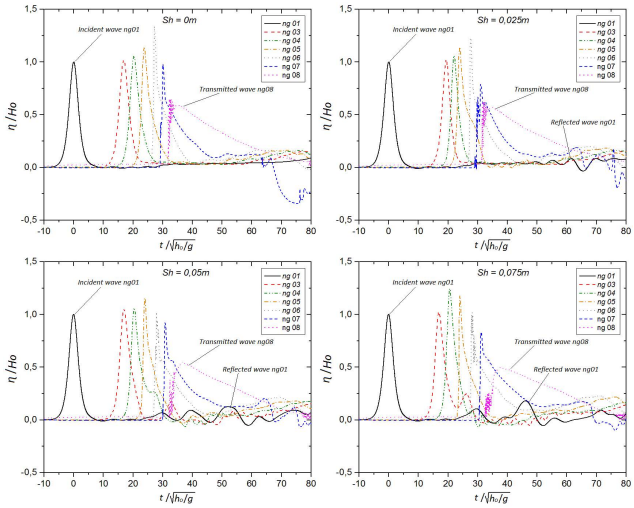

Fig. 7 Wave surface elevation time histories at the different numerical gauges (h_0=0.2m, H_0= 0.06m, slope 1:20).

To show the effect of slope on the breaking point, Fig. 8 present the elevation of the free surface at the moments of the breaking point for different slopes for water depth h_0=0.2m, wave height H_0= 0.06m, and stepped width Sw=1m, the increase in slope results from an increase of the stepped height Sh, for 1:15, 1:20, and 1:25, Sh is 0.025, 0.05, and 0.075m respectively see Fig. 1(b).

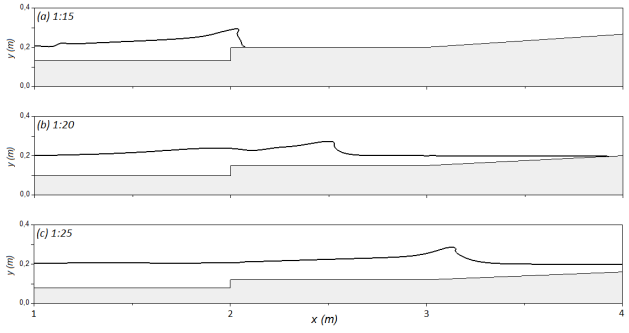

Fig. 8 Free surface elevation at the breaking point moments for different slope (h_0=0.2m, H_0= 0.06m, Sw=1m).

It is possible to figure out the breaking point location X_b, with the availability of detailed wave surface distribution data, it is clearly shown that milder slope caused the incipient wave breaking further shoreward Fig. 8c, and the rise of stepped height S_h caused an increase of the solitary wave height at breaking H_b Fig. 8(a).

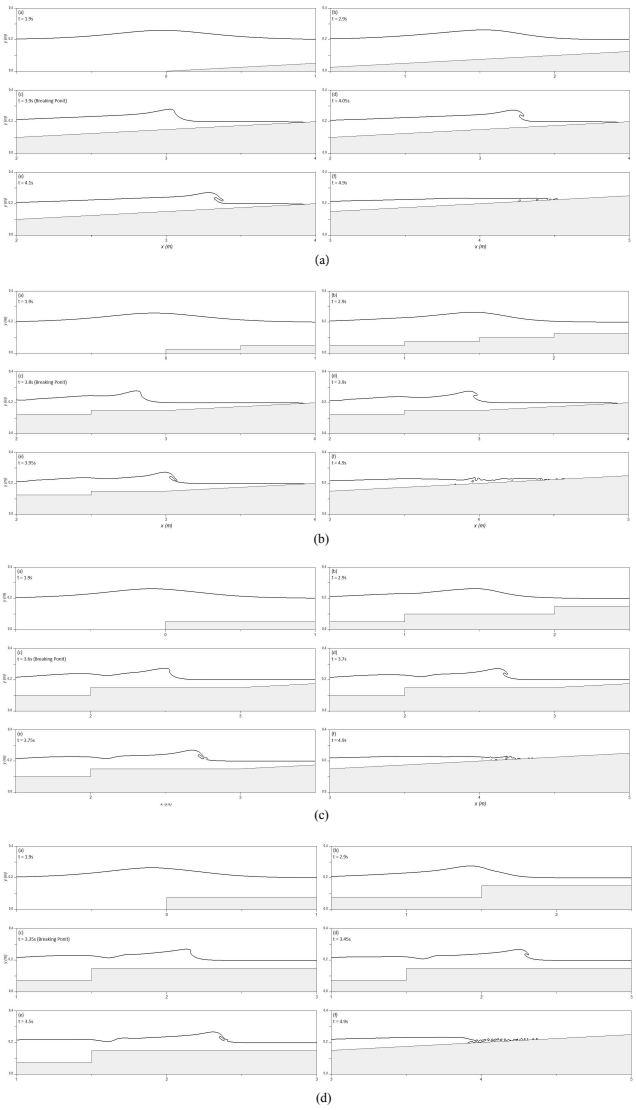

Fig. 9 Free surface elevation when the solitary wave propagates on the 1:20 slope , H_0= *0.06m* , h_0= *0.2m*. (a) *Sh =0m* , (b) *Sh= 0.025m ;* (c) *Sh= 0.05m ;* (d) *Sh= 0.075m*

Fig. 9. shows the changes in the wave surface profile during the shoaling and breaking process for the wave with H_0= *0.06m* at h_0 = *0.2m* on 1:20 slope for different step height *Sh*. The wave surface becomes unsymmetrical about the wave crest when the solitary wave arrives at the toe of the slop, as shown in Fig. 9(a)**.** As propagating the further steepening of wave-front causes the initiation of wave breaking process, the wave-front face develops into vertical and steeper with the decreasing local water depth Fig. 9(b,c). The position of the breaking point Xb decreases and the breaking phenomenon is in advance when the stepped height *Sh* increases Fig. 9(c).

After that, the wave crest continues to increase, then rolls down, and finally plunges into the water, as shown in Fig. 9(d,e)**.** The obtained geometric criterion of the breaking point form is consistent with those of Chen et al.[11] ; Grilli et al. [21] and Lin et al.[38] .

The breaking of the wave creates turbulence and tumbling of the water flow, the crest overturns with an ejecting water jet emanating, during wave curling down it entraps a large amount of air to form bubbles of different sizes, and the surge continues to propagate with the entrapped bubbles after the wave-front passes through the still-water shoreline, it collapses and the consequent run-up process commences, the surging starts earlier when the stepped height *Sh* rise, as shown in Fig. 9(f)**.**

It is noted that the present model is capable of capturing the plunging breaking, which means that the numerical method in this study can simulate wave breaking considerably well.

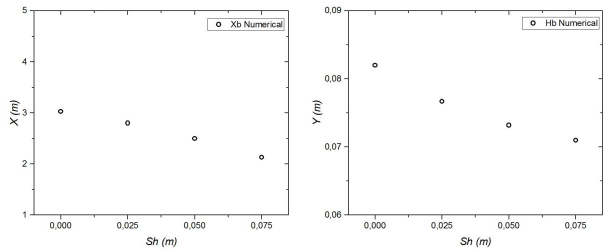

Fig. 10 Present numerical of the location of breaking point *Xb* (a) ; and solitary wave height at breaking *Hb* (b) for different stepped height *Sh*

The theatrical solitary wave height at breaking from the equation (13) for h_0= *0.2m,* H_0=

0.06m, slope *1:20* is $H_{b\ (\text{theatrical})} = 0.09$m compared with the present numerical solitary wave height at breaking without stepped structure (*Sh= 0m*) is $H_{b\ (numerical)} = 0.081m$, the maximum error of *Hb* value is 10%, and for *Xb* is 3% Fig. 6. It is shown the presence of stepped structures caused the reduction of the location of breaking point *Xb* nearly 1m for Sh= 0.075m Fig. 6a. However, a slight decrease of the wave height at breaking *Hb* was also observed, where an important portion of the incident wave could be reflected due to an increase of stepped height *Sh* Fig. 6(b).

4.3 Wave run-up, wave reflection, and wave transmission

The maximum run-up height of the wave is defined as the height from the still water level to the highest position where the wave arrives on the slope, we present numerical results for run-up, and evaluate the influence of incident wave height (H_0= *0.04, 0.06, 0.08m*), water depth (h_0=*0.15, 0.2, 0.25m*), beach slope (*ß= 1:15, 1:20, 1:25*), and step height (S_h= *0.025, 0.05, 0.075m)* on the maximum run-up height of the solitary wave.

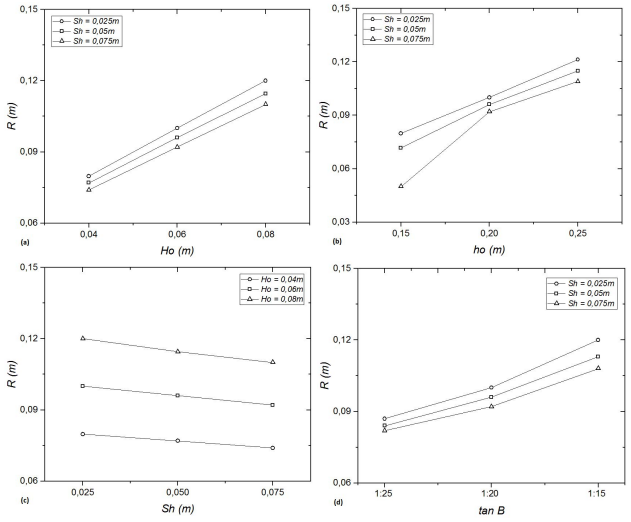

Fig. 11. Variations of maximum run-up on the slope with different: (a) wave heights; (b) water depths; (c) beach slopes; and (d) and step height.

The maximum run-up increased with increasing wave height H_o Fig. 11(a) also increased with increasing water depth h_o Fig. 11(b), due to the incident wave energy rose with the increase of wave height and water depth. The growth rate of the maximum run-up is greater when the beach slope is steeped and similarly when the wave height increases.

Fig. 11(c) shows the influence of the step height *Sh* (*Sh= 0.025, 0.05, 0.075m*) on the maximum run-up height of the solitary wave. The run-up decreases with increasing the step height *Sh* for all wave height. For the influence of the beach slope (*ß= 1:15, 1:20, 1:25*) Fig. 11(d). the run-up increases with increasing beach slope tan *ß* combined with increasing the step height *Sh*. With a steeper beach slope, the breaking wave cannot propagate on the slope, and run-up decreases with the beach slope (slightly step height *Sh*).

Measurement points were chosen to analyze wave reflection *Hr* at (ng01) and transmission *Ht* at (ng08). It is visible (see Fig. 7) the wave height at (ng08) decreases with increasing step height *Sh*, moreover, the numerical wave gauge (ng01) did not record any wave reflected for plane slope without stepped structure Fig. 6(a), however, the number and the height of reflected wave depending on step height Sh.

The reflected wave slightly decreased with increasing water depth Fig. 12(b), However, it decreased with the increase of wave height Fig. 12(a). The transmitted wave height decreased with increasing wave height, but it increased rapidly with increasing water depth Fig. 12(a,b).

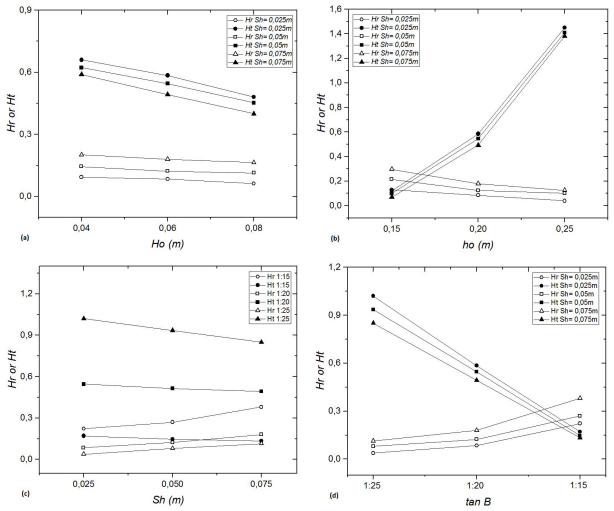

Fig. 12. Variations of simulated reflected wave height at (ng01) and transmitted wave height at (ng08) with different: (a) wave heights; (b) water depths; (c) beach slopes; and (d) and step height

For the effect of step height *Sh* and slope beaches on reflected and transmitted wave, it is clearly shown that increase of *Sh* cause slight decrees of transmitted wave Fig. 11(c). It is the same for slope beaches but decreasing rapidly due to combined with an increase of step height *Sh* Fig. 11(d). However, the reflected wave increase with increasing of step height *Sh* and slope beaches caused the incipient wave breaking closer to the toe of the slope.

The reflection coefficient is inversely proportional to the incident wave. Moreover, Yao et al.[29] declared decreasing of wave reflection with increasing beach slope was also observed with the presence of pile structure in slope, which is contrary to the case for wave interaction with a slope without the pile structure.

5 Conclusion

In this paper, solitary wave propagating on a sloping beach are investigated, a two-dimensional numerical model based on ANSYS Fluent was established. The Navier–Stokes equations with *k-ε* turbulence closure were solved and the free surface was tracked by a VOF method, a set of numerical simulations were implemented to investigate the water surface profile, shoaling and breaking of solitary waves , wave reflection, the wave transmission, and the wave run-up by varying incident wave height, water height, beach slope, and step height *Sh*.

- The results obtained from the Fluent solver simulations with a multiphase model for both *k-ε* are in corroboration with the empirical formulas for solitary wave run-up on the slope, also with numerical results and experimental data, indicate that the numerical model can accurately model the free surface elevation, the breaking processes and the maximum run-up for different slope beach.

- The breaking process dissipates energy in the form of turbulence, the variation of the step height *Sh* affects the location of breaking point *Xb* back close to the toe of the slope, and decrease of the wave height at breaking *Hb*, as well as the maximum run-up, so the run-up increases with increasing beach slope, wave height, and water depth.

- The wave reflection decreased with the increase of water depth, and wave height. Otherwise, increased slightly with increasing step height *Sh* and increased rapidly with beach slope. As well as the wave transmitted increased with the increase of water depth, and decreased with increasing wave height, step height, and beach slope.

References:

[01] A.C. Yalciner, A. Suppasri, E. Mas, N. Kalligeris, O. Necmioglu, , F. Imamura, C. Ozer, , A. Zaytsev, , N. M. Ozel, C. Synolakis, Field survey on the coastal impacts of March 11, 2011 great east Japan tsunami , *2012, Pure and Applied Geophysics (This volume).*

[02] J. Boussinesq, Théorie de l'intumescence liquide appelée onde solitaire ou de translation se propageant

dans un canal Rrectangulaire, *Comptes Rendus Acad. Sci. Paris, 1971, Vol 72, pp 755- 759.*

[03] J. B. Keller, The Solitary wave and periodic waves in shallow water, Commun. Appl. Math., 1948, Vol 1, pp 323-339.

[04] L. Rayleigh, On Waves, *Phil. Mag.,1876, Vol 1, pp 257-279.*

[05] W.H Munk, The Solitary wave theory and its application to surf problems, Annals New York Acad. Sci., 1949 , Vol 51, pp 376-423.

[06] J. D. Fenton, A ninth-order solution for solitary waves, *Jour. Fluid Mech.,* 1972 , *Vol 53, pp 257-271.*

[07] J. G. B. Byatt-Smith, M.S. Longuet- Higgins, On the speed and profile of steep solitary waves, *Proc. Roy. Soc. London, Series A, 1976, Vol 350, pp 175-189.*

[08] M. S. Longuet-Higgins, J. D. Fenton, On mass, momentum, energy, and calculation of a solitary wave, *Proc. Roy. Soc. London, Series A, 1974 ,Vol 340, pp 471-493.*

[09] S.C. Hsiao, T.C. Lin, Tsunami-like solitary waves impinging and overtopping an impermeable seawall: Experiment and RANS modeling, *Coastal Engineering 57 (2010) 1–18.*

[10] C. Jiang, X. Lü, Y. Yao, B. Deng, J. Chen, Numerical investigation of tsunami-like solitary wave interaction with a seawall, *Journal of Earthquake and Tsunami Vol. 11, No. 1 (2017) 1740006.*

[11] D. Cheng, X. Zhao, D. Zhang, Y. Chen, Numerical study of dam-break induced tsunami-like bore with a hump of different slopes, *China Ocean Eng., 2017, Vol. 31, No. 6, P. 683–692.*

[12] K. Shao, W. Liu, Y. Gao, Y. Ninga, The influence of climate change on tsunami-like solitary wave inundation over fringing reefs, *Journal of Integrative Environmental Sciences, 2019, VOL. 16, NO. 1, 71–88*

[13] K. Qu, X.Y. Ren, S. Kraatz, Numerical investigation of tsunami-like wave hydrodynamic characteristics and its comparison with solitary wave, Applied Ocean Research 63 (2017) 36–48.

[14] G. Cannata, L. Barsi, C. Petrelli, F. Gallerano, Numerical investigation of wave fields and currents in a coastal engineering case study, *WSEAS Transactions on Fluid Mechanics, Vol. 13, 2018, pp. 87–94.*

[15] Q. Ji, X. Liu, Y. Wang, C. Xu, Q. Liu , Numerical investigation of solitary waves interaction with an emerged composite structure, *Ocean Engineering 218 (2020) 108080.*

[16] P.D. Hieu, T. Katsutoshi, V.T. Ca, Numerical simulation of breaking waves using a two-phase flow model, *Applied Mathematical Modelling 28 (2004) 983–1005.*

[17] C.K. Ting Francis, T. Kirby James, Observation of undertow and turbulence in a laboratory surf zone, Coastal Engineering 24 (1994) 51-80.

[18] F. Dentale, G. Donnarumma, E.P. Carratelli, F. Reale, A numerical method to analyze the interaction between sea waves and rubble mound emerged breakwaters, *WSEAS Transactions on Fluid Mechanics, Volume 10, 2015, pp. 105-115*

[19] A. Khaware, V. Gupta, K. Srikanth, P. Sharkey, Sensitivity analysis of non-linear steep waves using VOF method, *Tenth International Conference on Computational Fluid Dynamics (ICCFD10), 2018, Barcelona, Spain,*

[20] L. Wu , Study on the tsunami force of the superstructures of the medium and small span bridges. *(MA.Eng Dissertation) Southwest Jiaotong University,2017, P.R. China*

[21] S.T. Grilli, I.A. Svendsen, R. Subramanya, Breaking criterion and characteristics for colitary waves on slopes, *J. Waterway, Port, Coastal, Ocean Eng. 1997.123:102-112.*

[22] S.C. Hsiao, T.W. Hsu, T.C. Lin, Y.H. Chang, On the evolution and run-up of breaking solitary waves on a mild sloping beach, *Coastal Engineering, 2008, 55(12), 975–988.*

[23] H. Akbari, . Simulation of wave overtopping using an improved SPH method, *Coastal Engineering, 2017, 126 (2017) 51–68.*

[24] F. Gallerano , G. Cannata , L. Barsi , F. Palleschi , B. Iele, Simulation of wave motion and wave breaking induced energy dissipation, *WSEAS Transactions on Fluid Mechanics, Volume 10, 2015, pp. 62-69.*

[25] N.T. Wu, H. Oumeraci, W. Partenscky, Numerical modelling of breaking wave impacts on a vertical wall, *1995, Coastal Engineering, pp 1672 - 1686.*

[26] C.R. Chou, K.Ouyang, The deformation of solitary waves on steep slopes, *Journal of the Chinese Institute of Engineers, 1999 , Vol. 22, No. 6, pp. 805-812.*

[27] P. Lin, K. Chang, L.F. Philip, Liu, Run-up and rundown of solitary waves on sloping beaches, J. Waterway, Port, Coastal, Ocean Eng, 1999 ,125:247-255.

[28] Y. Kuai, M. Qi, J. Li, , Numerical study on the propagation of solitary waves in the near-shore, *Ocean Engineering 165 (2018) 155–163.*

[29] Y. Yao, J. Mei-juna, M. Da-weib, D. Zheng-zhic, L. Xiao-jiana, A numerical investigation of the reduction of solitary wave runup by A row of vertical slotted piles, *China Ocean Eng.*, 2020, Vol. 34, No. 1, P. 10–20

[30] C.E. Synolakis, The runup of solitary waves, *Journal of Fluid Mechanics, 1987, 185, 523–545.*

[31] N.B. Kerpen, , T. Schlurmann, Stepped revetments – Revisited, *Proc. 6th Int. Conf. on the Application of*

Physical Modelling in Coastal and Port Eng. and Science (Coastlab16), 2016, Ottawa, Canada, 1-10.

[32] N.B. Kerpen, T. Schoonees, T. Schlurmann, Wave overtopping of stepped revetments, *Water 2019, 11, 1035.*

[33] R.S. Shih, W.K. Weng, C.Y Li, Characteristics of wave attenuation due to roughness of stepped obstacles, *Ships and Offshore Structures, 2020, 10.1080/17445302.2019.1661652.*

[34] W. Yang , Z. Wen, F. Li, Q. Li, Study on tsunami force mitigation of the rear house protected by the front house, *Ocean Engineering 159 (2018) 268–279.*

[35] P. Prabu, B.S. Murty, C. Abhijit, S.A. Sannasiraj, Numerical investigations for mitigation of tsunami wave impact on onshore buildings using sea dikes, *Ocean Engineering 187 (2019) 106159.*

[36] J. Zhan, J. Zhang, Y. Gong, Numerical investigation of air entrainment in skimming flow over stepped spillways, *Theoretical and Applied Mechanics Letters,2016, S2095-0349(16)30009-5.*

[37] D. John Fenton, The cnoidal theory of water waves, *Chapter 2 of Developments in Offshore Engineering, Ed. J.B. Herbich, Gulf: Houston, 1998.*

[38] Y. Li, F. Raichlen, Energy balance model for breaking solitary wave run-up, J. Waterway, *Port, Coastal, Ocean Eng. 2003.129:47-59.*